PHYSICAL REVIEW C VOLUME 13, NUMBER 4 APRIL 1976

Multistep inelastic processes in the reaction ^{28}Si(^{3}He, d)^{29}P leading to bound and unbound states*

L. Ray and W. R. Coker
Department of Physics, University of Texas, Austin, Texas 78712
(Received 8 December 1975)

We analyze the stripping reaction ^{28}Si(^{3}He, d)^{29}P at an incident ^{3}He energy of 35.3 MeV, considering seven residual states. These extend in excitation energy to 4.8 MeV with the highest four being unbound to proton emission and described via complex energy eigenstates. The results of a distorted-wave Born-approximation analysis are rather disappointing. Through a coupled-channel Born approximation analysis, inelastic excitation in both the entrance and exit channels is shown in several cases to be important in accounting for the detailed shape of the angular distributions. Additional data obtained at 20 and 40 MeV are included in the analysis as a check of the optical potentials and spectroscopic amplitudes adopted. The spectroscopic amplitudes used are consistent with results of large-basis shell-model calculations. Good fits to the (^{3}He, d) data are obtained in both shape and magnitude, suggesting that the coupled-channel Born approximation should replace the distorted-wave Born approximation in the analysis of experimental data for single-nucleon transfer reactions in this mass region.

[NUCLEAR REACTIONS ^{28}Si(^{3}He, d), E=20, 35.3, 40 MeV; DWBA and CCBA calculations of $\sigma(E_d, \theta)$. Deduced multistep inelastic contributions and spectroscopic amplitudes.]

I. INTRODUCTION

The use of (^{3}He, d) and (d, ^{3}He) reactions for detailed studies of the nuclear spectroscopy of proton particle and hole states began in earnest about ten years ago.[1] Since then, a vast number of studies have been carried out using these reactions, at nuclear science facilities all over the world.

In recent years, it has been realized that excitation of inelastic channels during nucleon transfer reactions can have important consequences; analysis of direct reaction cross section data using the conventional distorted-wave Born approximation (DWBA) can lead to erroneous spectroscopic conclusions, and fails to account for many remarkable, systematic features of the angular distributions.[2]

The (^{3}He, d) reaction has also been used frequently to explore the low-lying proton continuum. Data for (^{3}He, d) to proton-unbound states has generally been analyzed in terms of ordinary DWBA with weakly bound states as residual nuclear form factors. Again, in recent years it has been realized that, even for proton resonances of width 10^{-5} MeV or less, use of a weakly bound state form factor in DWBA can lead to erroneous conclusions.[3,4]

In the present work we discuss an analysis in which both of these difficulties are present. The reaction ^{28}Si(^{3}He, d)^{29}P has been studied at 35.3 MeV incident ^{3}He energy by Leleux *et al.*[5] From previous coupled-channel Born approximation (CCBA) analyses of the mirror reaction ^{28}Si(d, p)-^{29}Si, it is known that inelastic excitation in entrance and exit channels has an important effect on certain transitions to states with small single-particle spectroscopic factors.[6] Further, a number of the states observed by Leleux *et al.* are unbound to proton emission.

Angular distributions are available covering center of mass angles from 10 to 70° for the following states in ^{29}P: $\frac{1}{2}^+$ ground, $\frac{3}{2}^+$ 1.38 MeV, $\frac{5}{2}^+$ 1.95 MeV, $\frac{5}{2}^+$ 3.1 MeV, $\frac{7}{2}^-$ 3.45 MeV, $\frac{3}{2}^-$ 4.34 MeV, and $\frac{1}{2}^+$ 4.76 MeV. The last four of these states are unbound to proton emission.[5]

Because of magnitude anomalies, to be discussed in the next section, we have also included in our analysis data for the ^{29}P ground state and the first excited state at 1.38 MeV obtained at incident ^{3}He energies of 20 MeV by Mertens, Mayer-Böricke, and Kattenborn[8] and at 40 MeV by Stupin, Ristenen, and Schwandt.[9]

These data have been analyzed in terms of the CCBA[2] using complex-energy eigenstates[7] to describe the unbound final nuclear states. To the best of our knowledge, this is the first instance of a CCBA description of direct reactions to unbound final states. In Sec. II we present the details of the analysis, and in Sec. III we draw conclusions.

In the CCBA analysis we have considered a number of alternate couplings in both entrance and exit channels, and have also made a study of the sensitivity of our results to variations in the relative phases of configurations contributing to parti-

cular final states. As a further point of interest, we have sought for evidence of $l = 2\,j$ dependence in the angular distributions for the $\frac{3}{2}^+$ 1.38 MeV and $\frac{5}{2}^+$ 1.95 MeV states in ^{29}P.[5,10] We expect that, as noted earlier,[6] inelastic effects are able to account in a very natural way for this hitherto unexplained total angular momentum dependence of the cross sections.

Our conclusions concerning the relative importance of various possible inelastic transitions, and the relative and absolute magnitudes of the spectroscopic amplitudes for the residual nuclear states, are in general agreement with and support the conclusions of an earlier, independent, study of the reaction ^{28}Si$(d,p)^{29}$Si in terms of the CCBA.[6]

II. CCBA ANALYSIS

The inputs needed for the CCBA analysis are the optical potentials, collective coupling parameters β_l, and spectroscopic amplitudes A_{lsj}. The formulation of CCBA we have used is that of Abdallah, Udagawa, and Tamura.[2] The states in ^{28}Si which are assumed to be relevant in the calculations are the 0^+ ground state, the 1.78 MeV 2^+ state, assumed here to be substantially a one-quadrupole-phonon state, and the 6.88 MeV 3^- state, assumed to be a one-octupole-phonon state. The $0^+ \rightarrow 2^+$ transition is given a role in the excitation of all the positive parity states considered in ^{29}P, whereas the $0^+ \rightarrow 3^-$ transition is included for the negative parity states considered in ^{29}P.

A number of studies utilizing both coupled channels[11,12] and DWBA[13-17] have been carried out for inelastic scattering from ^{28}Si. On the basis of these analyses, we adopt a value of $\beta_2 = 0.40$ for the $0^+ \rightarrow 2^+$ transition,[15,16] while for the $0^+ \rightarrow 3^-$ coupling we use $\beta_3 = 0.45$.[16,17] For the $\Delta L = 2$ inelastic transitions in ^{29}P we use a value $\beta_2 = 0.35$, following Coker, Udagawa, and Hoffman,[6] while for the $\frac{1}{2}^+ \rightarrow \frac{7}{2}^-$ coupling we adopt the value $\beta_3 = 0.37$ obtained by Crawley and Garvey.[18]

The optical model parameters used in the DWBA calculations are those suggested by Coker[19] on the basis of a DWBA analysis of ^{28}Si$(^3$He$,d)^{29}$P ($\frac{1}{2}^+$ ground state) over a wide range of incident energies. These parameters not only give good fits to the elastic scattering data at energies relevant to the present analysis, but also yield energy-independent spectroscopic factors in a DWBA analysis of the ^{28}Si$(^3$He$,d)$ reaction from 18 to 40 MeV incident ^{3}He energy.[19] In the standard notation V, W, W_D, V_{so}, r, a, r', a', r_{so}, a_{so}, the ^{3}He parameters are 147.6, 30.9, 0.0, and 3.0 MeV, 1.16, 0.72, 1.49, 0.83, 1.16, and 0.72 fm; the d parameters are 108.2, 0.0, 20.8, and 12.0 MeV, 1.07, 0.858, 1.488, 0.535, 0.955, and 0.500 fm. The ^{3}He optical potential is that obtained by Leleux,[5] from a direct fit to the 35 MeV ^{3}He-^{28}Si elastic scattering, while the d parameters are taken from the Perey-Perey tabulation.[20] The Coulomb radius r_C was taken as 1.3 fm in both ^{3}He and d channels.

When explicitly including inelastic channels, via solution of coupled equations, one expects in general to have to alter or "renormalize" the elastic-channel optical model potential in order to recover a satisfactory fit to the elastic scattering. This is particularly important in the present calculations, because we have in addition excluded spin-orbit coupling in all our CCBA calculations. This was done since a number of previous DWBA and CCBA studies indicate that the spin-orbit effects are unimportant in accounting for the detailed shape or magnitude of the angular distributions for (d,p) and $(^3$He$,d)$ reactions in this mass region,[3,6,19] and exclusion of spin-orbit coupling from the CCBA calculations results in nearly an order-of-magnitude saving in computer time. Thus we have required that the optical potentials we use in our CCBA calculations reproduce the elastic scattering not only with explicit coupling to inelastic channels, but also with the spin-orbit terms set to zero. The new potentials were found using the coupled-channel program JUPITOR I, written by Tamura.[21]

In the ^{3}He-^{28}Si channels, the effect of inelastic coupling was considerably more important than the neglect of the (already small) spin-orbit term. For $0^+ \rightarrow 2^+$ coupling, it was necessary to increase W from 30.9 to 40.0 MeV, neglecting the spin-orbit terms, to recover the original fit to elastic scattering. For the $0^+ \rightarrow 3^-$ coupling in ^{28}Si, no change in the original ^{3}He potential was required, with or without the spin-orbit term.

In the $d + ^{29}$P exit channels, as one would expect, the neglect of the spin-orbit term had a much greater effect than in the ^{3}He$+^{28}$Si case. Indeed, the effect of neglect of the spin-orbit potential was greater than the effect of the inelastic coupling. We recovered the original fit to the elastic scattering data by decreasing the well depth of the real potential from 108.2 to 95.0 MeV, almost independent of the inelastic couplings included.

These results are summarized in Fig. 1, where the solid curve shows the original optical model prediction for the elastic scattering, including spin-orbit coupling, for both ^{3}He and d potentials. The dashed curves show the coupled-channel predictions for the elastic scattering, with the spin-orbit terms omitted but the original potentials otherwise unchanged. Finally, the dot-dash curves show the coupled-channel predictions with all the corrections discussed above. It is seen that the original cross sections are rather well reproduced. These adjusted optical model parameters were

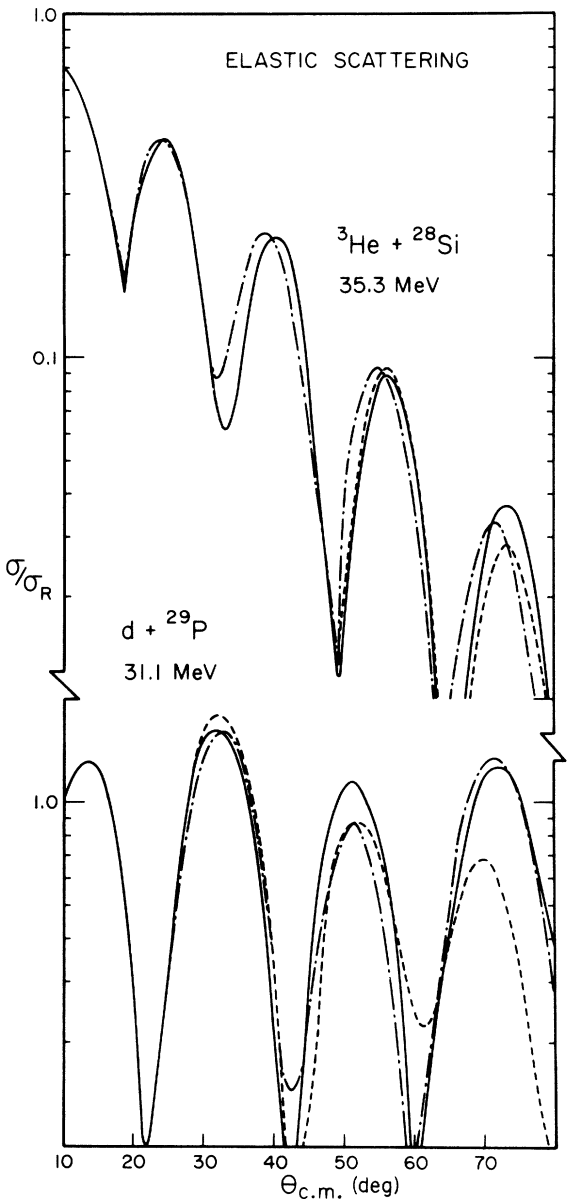

FIG. 1. The ^{3}He + ^{28}Si and d + ^{29}P elastic scattering angular distributions. The solid curves represent uncoupled optical model calculations including the spin-orbit force. The uncorrected coupled equation solutions with no spin-orbit force are shown by the dashed lines where $0^+ \rightarrow 2^+$ coupling in ^{28}Si and $\frac{1}{2}^+ \rightarrow \frac{3}{2}^+$ coupling in ^{29}P are assumed. The coupled-channel solutions with no spin-orbit force and with the corrections as discussed in the text are represented by the dash-dot curves. Other couplings in ^{29}P give essentially identical cross sections as those shown here.

used in all the CCBA calculations reported here for 20, 35.3, and 40 MeV incident ^{3}He energies.

It is interesting that the neglect of the spin-orbit terms had in general a greater or about the same effect as explicit inclusion of inelastic excitations. In our experience[6] this is not an unusual circumstance for vibrational coupling. For rotational coupling, on the other hand, consequences are rather more extreme.[2]

The CCBA calculations were performed using a specially modified version of the program MARS.[22] Changes were made to accommodate the complex-energy eigenstates (Gamow states) used to describe the ^{29}P proton resonances, and to carry out the Abel regularization procedure with a weighting function $\exp(-\alpha r^2)$ as discussed by Coker and others.[7] The potential parameters used for both the bound and Gamow states were fixed at $V_{so} = 6.0$ MeV, $r = r_{so} = r_C = 1.18$ fm, $a = a_{so} = 0.73$ fm. The real-well depth was adjusted to produce a bound state at the experimental separation energy, or a single-particle resonance at the experimental excitation energy. The resonance energy E_R, single-particle width Γ_{sp}, and Woods-Saxon well depth obtained are listed in Table I for each ^{29}P state.

Due to core limitations, only 24 partial waves were used in the majority of the CCBA calculations. However, for these transitions in DWBA the increase to 35 partial waves changes the direct cross sections by only 10^{-3}. Since the direct process is dominant in all but one of the transitions studied, these truncation errors are therefore negligible. Because of the large incident energy, we have also neglected Coulomb excitation. Furthermore, the difficulties encountered at back angles with compound nucleus contributions to the reaction cross sections[23] for the low energy ^{28}Si-(d,p) studies[6] do not appear here.

We have assumed vibrational coupling throughout; the states in ^{29}P are assumed to be populated either directly from the ground state of ^{28}Si by proton stripping, indirectly following inelastic excitation of ^{28}Si through $[^{28}\text{Si}^* \otimes s_{1/2}]$ or $[^{28}\text{Si}^* \otimes d_{3/2}]$ weak-vibrational-coupling components of the ^{29}P

TABLE I. Resonance energy E_R, single-particle width Γ_{sp}, and Woods-Saxon well depth for each ^{29}P state.

State	E_R (MeV)	Γ_{sp} (keV)	V_{binding} (MeV)
$\frac{1}{2}^+$ g.s.	...	...	53.7
$\frac{3}{2}^+$ 1.38 MeV	...	...	56.1
$\frac{5}{2}^+$ 1.95 MeV	...	...	46.8
$\frac{5}{2}^+$ 3.10 MeV	0.36	2.2×10^{-5}	44.3
$\frac{7}{2}^-$ 3.45 MeV	0.70	7.3×10^{-4}	67.5
$\frac{3}{2}^-$ 4.34 MeV	1.60	76.0	64.7
$\frac{1}{2}^+$ 4.76 MeV	2.02	470	40.3

states, or indirectly via inelastic excitation from the ground state of ^{29}P. In general, all three paths are allowed.

In the CCBA calculations, therefore, we need three single-nucleon transfer spectroscopic amplitudes A^i_{lsj}. A^1 is, in our convention,[6] the amplitude for ground-state to ground-state stripping, which can be obtained from DWBA or CCBA fits to the ^{28}Si(^{3}He, d)^{29}P($\frac{1}{2}^+$ ground state) data. A difficulty occurs in the present case which was not encountered in previous analyses[6,24] and will be discussed in detail below. A^2 is the amplitude for the transition from an excited state of ^{28}Si—in our calculations always the 1.78 MeV 2^+_1 or the 6.88 MeV 3^-_1—to the given state in ^{29}P. In our weak-coupling picture, this amplitude when not zero is set equal to the amplitude for direct stripping to the lowest-lying $s_{1/2}$ or $d_{3/2}$ state in ^{29}P. Finally, A^3 is the amplitude for the direct stripping transition from the ground state of ^{28}Si to the specific final state of ^{29}P considered. In the conventional (DWBA) situation, $A^1 = A^2 = 0$, A^3 would be expected to be simply the square root of the DWBA spectroscopic factor for the ^{29}P state.

Our philosophy is that these amplitudes should be determined in a reasonably self-consistent way; certain difficulties, however, must be faced in analyzing the present data. In each CCBA calculation we obtain all the cross sections for the final states which we assume to be inelastically coupled simultaneously. Thus, an angular distribution for the ^{28}Si(^{3}He, d)^{29}P($s_{1/2}$, g.s.) transition is calculated during each and every CCBA calculation performed for any final state in ^{29}P. All our calculations, both DWBA and CCBA, use the same value for the (^{3}He, d) zero-range interaction strength, $D_0^2 = 3 \times 10^4$ MeV^2 fm^3.[1] With this value of D_0 and the chosen optical model potentials, the DWBA spectroscopic factor obtained for the ground state of ^{29}P agrees well with the shell model predictions.[19,25] However, it was found that if A^1 is the spectroscopic amplitude which fits the ground-state cross section in DWBA, this cross section in CCBA is invariably overestimated by nearly a factor of 1.3. Such a situation did not occur in the ^{28}Si(d, p) analysis, where there was no significant difference between CCBA and DWBA predictions for the ^{29}Si ground state.[6] The DWBA analysis of ^{28}Si(^{3}He, d) yields a spectroscopic factor of about 0.46, and thus an amplitude of 0.68, comparing well to the value of 0.73 obtained in Ref. 6. However, to obtain the correct ground-state cross section in CCBA requires in this case a reduction of the amplitude to 0.60, corresponding to a ground-state spectroscopic factor of only 0.36; the shell model prediction[25] is 0.5. Furthermore, the value of 0.60 also predicts the correct magnitude for the ground-state cross sections at 20 and 40 MeV incident energy.

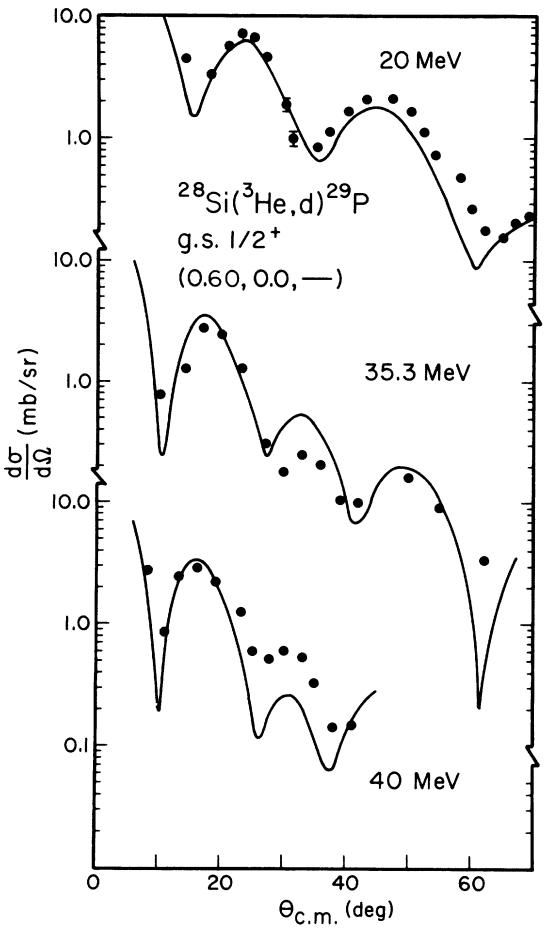

FIG. 2. The ^{28}Si(^{3}He, d)^{29}P angular distributions at 20, 35.3, and 40 MeV incident ^{3}He energy populating the ground state. Errors are statistical and are smaller than the size of the data points. The solid curve for the 35.3 MeV data is the result of a CCBA calculation in which the 1.95 MeV $\frac{5}{2}^+$ second excited state is considered as discussed in the text. The other two result from 1.38 MeV $\frac{3}{2}^+$ coupling with the ground state. The amplitude given is that of the ground state to ground state transition. (See the discussion in the text of the 1.95 MeV $\frac{5}{2}^+$ state for details of the coupling involved).

We have therefore of necessity used the value of 0.60 for all of the CCBA calculations reported here. The solid lines in Fig. 2 show typical CCBA calculations with $A^1 = 0.60$ for all three energies. They are quite similar to a DWBA calculation with $A^1 = 0.7$.[5,6] The amplitude A^2 for transition to the $d_{3/2}$ first excited state of ^{29}P is similarly fixed at 0.86 by DWBA analysis of the 1.38 MeV $\frac{3}{2}^+$ angular distributions as shown in Fig. 3. This amplitude corresponds to a spectroscopic factor of 0.74, in fair agreement with the shell-model prediction of 0.6.[25] As is seen in Fig. 3, an excellent fit in both

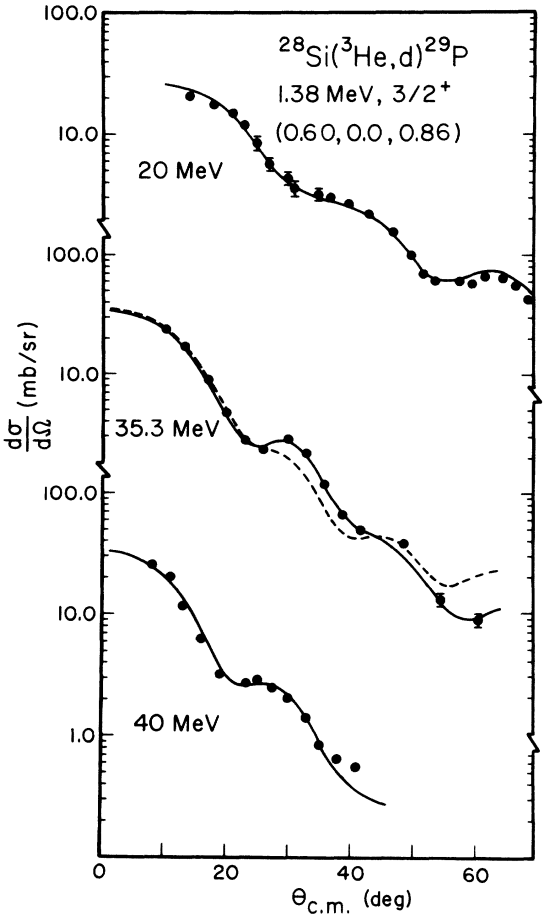

FIG. 3. The ^{28}Si(^{3}He,d)^{29}P cross sections leading to the $\frac{3}{2}^{+}$ first excited state at 1.38 MeV for ^{3}He energies of 20, 35.3, and 40 MeV. Experimental errors are smaller than the data points unless otherwise indicated. The best CCBA calculations are represented by the solid curves while the DWBA prediction is shown by a dashed curve. The set of three numbers is (A^1, A^2, A^3) as discussed in the text and given in Table II. Notice the evidence of j dependence in the data near 50° c.m.

shape and magnitude is obtained at 20, 35, and 40 MeV incident energies. In this figure, and all subsequent figures, the 35 MeV data has been increased in absolute magnitude by a factor of 2.2. If this is not done, the 35 MeV data for all excited states of ^{29}P are consistently too low in absolute magnitude, as compared to the 40 MeV data, by a factor of 1/2.2. Furthermore, spectroscopic amplitudes extracted from the original 35 MeV data for all excited states are a factor 1/2.2 too low, in *both* DWBA and CCBA, compared to those resulting from analysis of (^{3}He,d) data at other energies, (d,p) data to the mirror states,[6] and shell-model predictions.[25] The factor of 2.2 was determined by direct comparison of the experimental data at 35 and 40 MeV. Once A^1 and A^2 are settled and the 35 MeV data are properly normalized, A^3 presents little problem. We find that within 20%, the value of A^3 can in fact be set equal to the square root of the shell-model or DWBA spectroscopic factor for the particular final ^{29}P state considered. Since DWBA does not provide a good fit to the angular distribution in many cases,[5] there is an ambiguity in the fitting procedure which is already greater than 20%. In short, given a previous DWBA analysis, our CCBA analysis turns out to have only one adjustable parameter A^1, which we in fact kept fixed throughout the calculation.

For each angular distribution we made a calculation using the "accepted" parameters, and then a series of other calculations in which one or more of the indirect paths was suppressed or altered. We now turn to a state-by-state discussion of the results.

Table II summarizes the spectroscopic amplitudes used in the calculations. Figs. 2–8 show the results of the calculations. Here, in each figure, the solid curve is the best CCBA prediction, while the dashed curve is the equivalent DWBA prediction. For unbound final states, Gamow states are used in both DWBA and CCBA. The spectroscopic amplitudes are summarized on each figure in the format (A^1, A^2, A^3) for ready reference. Note that throughout Figs. 3–8, the data of Leleux *et al.* have been increased in absolute strength by a factor of 2.2.

As can be seen from Figs. 2–4, the angular distributions for the ground state, first excited, and second excited states of ^{29}P are well described by the CCBA calculations, which are a noticeable improvement over the DWBA results shown as dashed lines in the latter two cases. Each CCBA calculation gives essentially identical fits to the ground state at all three energies, in both shape and magnitude, provided we take $A^1 = 0.60$. In Fig. 2, we show CCBA predictions at 20, 35.3, and 40 MeV, using identical optical potentials, spectroscopic amplitudes, and inelastic coupling parameters in each case. The particular ground-state angular distribution shown is that obtained along with the angular distribution for the 1.95 MeV $\frac{5}{2}^{+}$ second excited state shown in Fig. 4, and discussed in a later paragraph. An effort was also made to fit the ground-state data with ($0^{+} - 2^{+}$) and ($\frac{1}{2}^{+} - \frac{3}{2}^{+}$) entrance and exit channel coupling, with all four possible transitions being allowed, and a rather poor fit was obtained.

In Fig. 3 we show the best CCBA descriptions of the first, 1.38 MeV $d_{3/2}$ state angular distributions at 20, 35.3, and 40 MeV. Again, we emphasize that these calculations are made essentially without adjustable parameters. The good description

TABLE II. Spectroscopic amplitudes for single proton transfer in $^{28}Si(^3He,d)^{29}P$.

Transition Initial	Final	l_j	$S(^3He,d)$ DWBA	$S(^3He,d)$ [a] CCBA	S_{theo} [b]	A_{lsj}
0^+ g.s.	$\frac{1}{2}^+$ g.s.	$s_{1/2}$	0.46	0.36	0.5	0.60
0^+ g.s.	$\frac{3}{2}^+$ 1.38 MeV	$d_{3/2}$	0.64	0.74	0.6	0.86
0^+ g.s.	$\frac{5}{2}^+$ 1.95 MeV	$d_{5/2}$	0.13	0.14	0.11	0.38
0^+ g.s.	$\frac{5}{2}^+$ 3.10 MeV	$d_{5/2}$	0.078	0.11	0.02	0.33
0^+ g.s.	$\frac{7}{2}^-$ 3.45 MeV	$f_{7/2}$	0.40	0.52	...	0.72
0^+ g.s.	$\frac{3}{2}^-$ 4.34 MeV	$p_{3/2}$	0.31	0.40	...	0.63
0^+ g.s.	$\frac{1}{2}^+$ 4.76 MeV	$s_{1/2}$	0.57 [c]	...	0.01	~ 0 [c]
2^+ 1.78 MeV	$\frac{5}{2}^+$ 1.95 MeV	$s_{1/2}$	...			0.60
2^+ 1.78 MeV	$\frac{5}{2}^+$ 3.10 MeV	$d_{3/2}$	...			0.86
2^+ 1.78 MeV	$\frac{1}{2}^+$ 4.76 MeV	$d_{3/2}$	...			0.86
3^- 6.88 MeV	$\frac{3}{2}^-$ 4.34 MeV	$d_{3/2}$	...			0.86

[a] Obtained from CCBA transition amplitude $A^{(3)}$.
[b] See Ref. 25.
[c] See text.

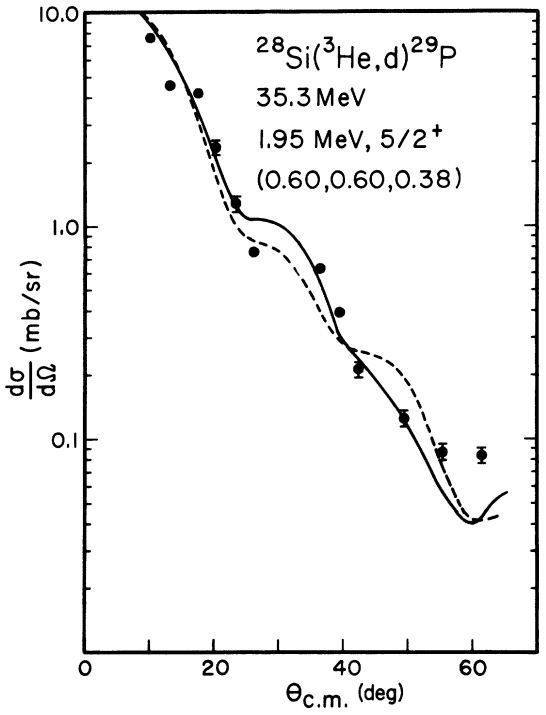

FIG. 4. Angular distribution for the 1.95 MeV $\frac{5}{2}^+$ bound state. The solid curve represents the best CCBA calculation and the dashed curve the DWBA result. Notice that all three routes are allowed to contribute in this case. This $l = 2$ state exhibits the usual j dependence in the data near 50° c.m.

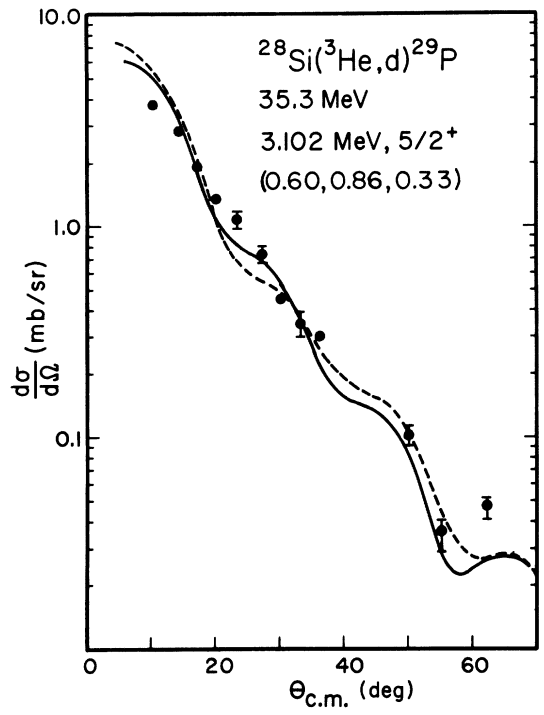

FIG. 5. Cross section for the $\frac{5}{2}^+$ proton unbound state at 3.10 MeV excitation energy in ^{29}P. Again all couplings are allowed to contribute to the final state in this best CCBA prediction (solid curve). The DWBA is shown by the dashed curve.

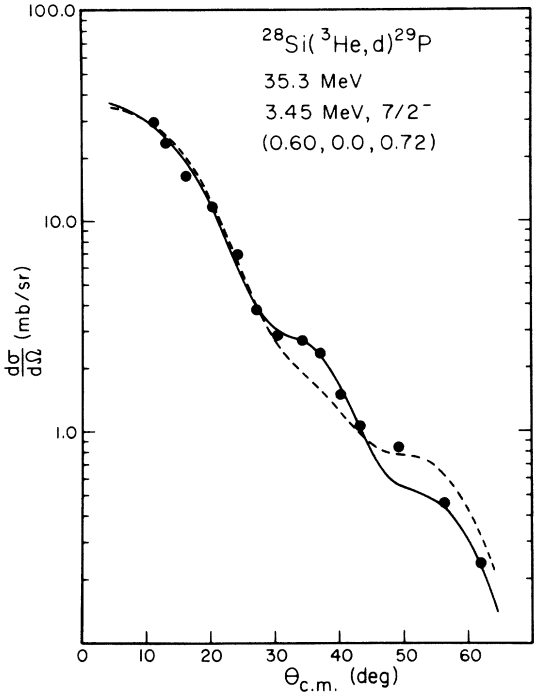

FIG. 6. The angular distribution for the ^{28}Si(^{3}He,d)^{29}P reaction leading to the $\frac{7}{2}^-$ unbound state at excitation energy 3.45 MeV. Note that entrance channel coupling is omitted in the CCBA calculation (solid curve). Here we see that the inelastic effects though rather small are exactly reflected in the data. Again the dashed line shows the DWBA result.

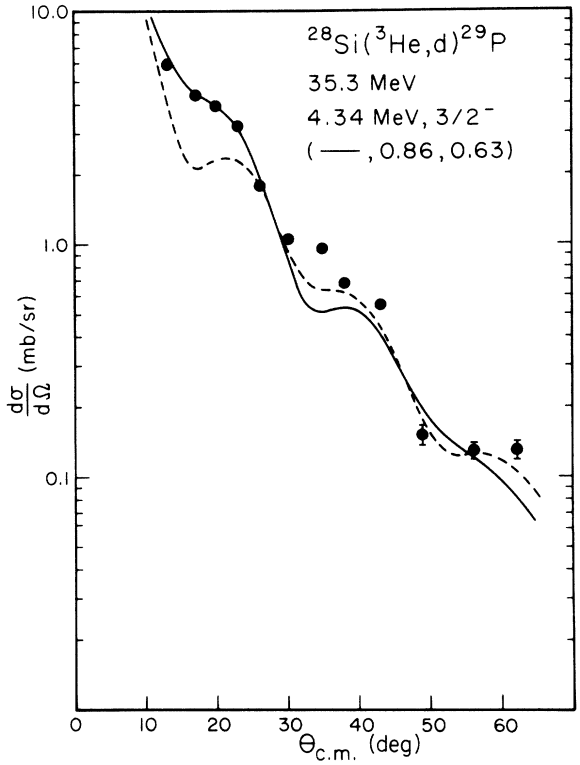

FIG. 7. The cross section for the $\frac{3}{2}^-$ unbound state at 4.34 MeV. Here the best CCBA fit (solid curve) involves only entrance channel excitation along with the direct component. The DWBA prediction as shown by the dashed curve is rather poor in comparison.

of these angular distributions seen in Fig. 3 results from inclusion of exit channel inelastic excitation only, as expected, since nuclear structure calculations do not suggest any important [(2$^+$, 1.78 MeV)$\otimes s_{1/2}$] component for this state. This result is also consistent with the earlier ^{28}Si(d,p) analysis.[6] Note particularly the improved fit past 50° center of mass.

On the other hand, the 1.95 MeV $d_{5/2}$ state's angular distribution, only available at 35.3 MeV as shown in Fig. 4, is nicely described in CCBA by inclusion of a [(2$^+$, 1.78 MeV)$\otimes s_{1/2}]_{5/2^+}$ configuration, such that $A^1 = A^2$. The jog in the experimental data at 15° is unlikely, and probably accounted for by experimental error. We have increased slightly the value of the direct amplitude A^3 used in the CCBA calculations, relative to that obtained via DWBA, by about 5%, this being well within experimental uncertainties. The effects of CCBA for this case become significant at 30° center of mass and beyond, and therefore only a very slight improvement over the DWBA prediction, again shown as a dashed line, is seen even at back angles.

The $d_{3/2}$ and $d_{5/2}$ state angular distribution shown in Figs. 3 and 4 seem to exhibit the characteristic (^{3}He,d)$l = 2j$ dependence, though not so clearly as in earlier data of Kattenborn, Mayer-Böricke, and Mertens.[10] The difference in the two experimental angular distributions near 50° is apparent. It is also clear that the CCBA calculations account well for the difference. For a fuller discussion of this point, with a variety of examples, see Refs. 6 and 24.

The first unbound state which we consider is the $\frac{5}{2}^+$ at 3.10 MeV. The entrance channel coupling assumed is through a [^{28}Si(2$_1^+$)$\otimes d_{3/2}]_{5/2^+}$ term in the residual nuclear wave function. This component was estimated to be the dominant one, rather than [^{28}Si(2$_1^+$)$\otimes s_{1/2}]_{5/2^+}$, on the basis of coupled-channel calculations using the program NEPTUNE.[26] In NEPTUNE, the configuration mixing of the Woods-Saxon single-particle basis states coupled to various core-excited vibrational states is calculated using the same ^{28}Si $\beta_{2,3}$ values used in MARS for the CCBA predictions.[27] In addition, the angular distribution is best fitted with an exit channel coupling of $\frac{1}{2}^+$ g.s. $-$ 3.10 MeV $\frac{5}{2}^+$, rather than, say, 1.38 MeV $\frac{3}{2}^+ -$ 3.10 MeV $\frac{5}{2}^+$. The direct transition amplitude A^3 needed is slightly larger than the

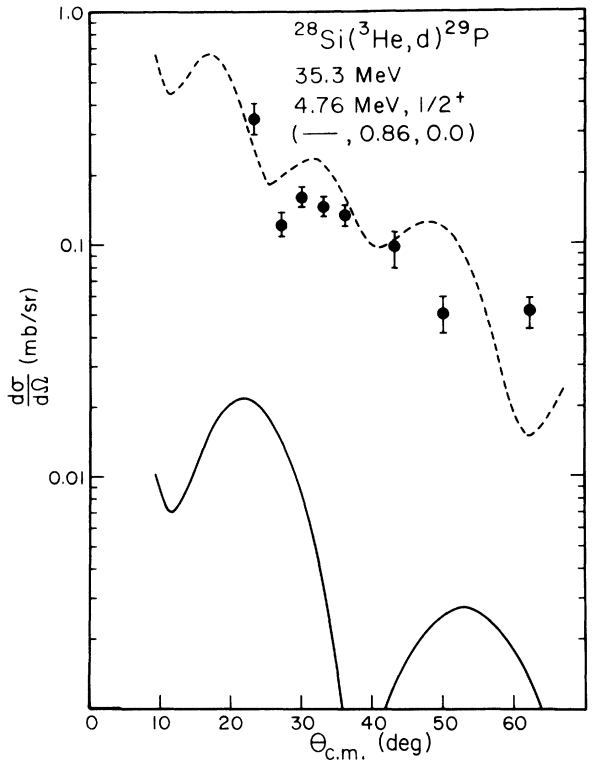

FIG. 8. The ^{28}Si(^{3}He,d)^{29}P reaction cross section populating the $\frac{1}{2}^{+}$ state at 4.76 MeV. The dashed curve represents the simple DWBA prediction while the solid curve gives the result of a CCBA calculation including only the entrance channel two-step process with no direct contribution included.

value of $[S(^{3}\mathrm{He},d)]^{1/2}$ determined via DWBA, but is well within experimental absolute-cross-section errors, as well as being within the range of ambiguity in the comparison of the poorly fitting DWBA calculation with the experimental angular distribution. Alternate calculations in which entrance channel excitations were deleted and in which the phase of A^3 was flipped gave very poor agreement with the data. Note that multistep effects are quite small in this case due to the high excitation energy, but that there is a slight improvement in the slope of the angular distribution at forward angles, as seen in Fig. 5.

Figures 6 and 7 show the DWBA and CCBA fits for the only two negative parity states considered in this analysis, the 3.45 MeV $\frac{7}{2}^{-}$ and 4.34 MeV $\frac{3}{2}^{-}$ resonances. Again, calculations with NEPTUNE assuming vibrational core coupling suggested that the $\frac{3}{2}^{-}$ state had a significant $[^{28}\mathrm{Si}(3_1^{-})\otimes(d_{3/2})]_{3/2^{-}}$ component. Further, the 3^{-} state at 6.88 MeV in ^{28}Si is the only negative parity state below 8.3 MeV in excitation energy; this lack of a number of minor competing paths presumably results in the extremely good fits obtained by CCBA for both of the negative parity states considered in ^{29}P. Conversely, the goodness of fit obtainable for the positive parity states of Figs. 3–5 is limited by our neglect of several possible small components of the residual state.[28]

Calculations for the $\frac{7}{2}^{-}$ state included a number of alternate assumptions: $[^{28}\mathrm{Si}(3^{-})\otimes s_{1/2}]_{7/2^{-}}$ coupling in entrance channel, along with exit channel coupling; no entrance channel coupling; and no exit channel coupling. The best fit was obtained for exit channel coupling only, $\frac{1}{2}^{+}$ g.s. $\rightarrow \frac{7}{2}^{-}$. On the other hand, the best fit for the $\frac{3}{2}^{-}$ state is obtained with entrance channel coupling only. A calculation including 1.38 MeV $\frac{3}{2}^{+} \rightarrow$ 4.34 MeV $\frac{3}{2}^{-}$ exit channel coupling made the quality of the fit much worse, aside from being a rather unlikely transition. For both negative parity states, the direct amplitudes A^3 were increased slightly over the values estimated from DWBA analyses, but again remained within the over-all uncertainty. Finally, a smaller value of β_3 was used in the entrance channel, 0.29,[15] with again poorer fits obtained. It is clear that the experimental angular distributions do show small but relatively unambiguous signs of multistep contributions, and small departures from the accepted parameters do not yield a good description of the data. Again, notice in Figs. 6 and 7 the improvement in the $\frac{7}{2}^{-}$ fit at all angles, and in the $\frac{3}{2}^{-}$ fit up to 30°.

The angular distribution for the $\frac{1}{2}^{+}$ state of 4.76 MeV shown in Fig. 8 presents special problems. The cross section for population of this state is more than an order of magnitude less than for any other transition considered. It seems *a priori* unlikely that a direct process plays a significant role in population of the state. Assuming a configuration including $[^{28}\mathrm{Si}(2_1^{+})\otimes d_{3/2}]_{1/2^{+}}$, we made CCBA calculations in which all three paths were considered simultaneously, and with one at a time deleted. None of these calculations gave a shape or magnitude comparable to the experimental data; indeed, the DWBA alone gave the best shape fit, as seen in Fig. 8. Our conclusion is that the state is not populated by a direct reaction mechanism to any significant degree; the great variety of possible indirect mechanisms preclude any further analysis, since no one of them could dominate the others significantly. Shown in Fig. 8 are the DWBA as a dashed curve, and the CCBA with no direct transition.

III. CONCLUSIONS

For all the transitions we have considered except the one populating the $\frac{1}{2}^{+}$ 4.76 MeV state, the direct stripping process plays a dominant role. Yet it is clear that the data do show reasonably characteristic features associable with indirect

processes through inelastic excitation in entrance and/or exit channels. While the DWBA is adequate to obtain orbital angular momentum transfer assignments and spectroscopic factors, it does not satisfactorily account for the detailed features of the experimental angular distributions. On the other hand, inclusion of the most important inelastic processes provides an immediate improvement in the fit to the angular distribution, without greatly upsetting the original conclusions of the DWBA analyses—which after all agree fairly well with extensive shell-model calculations.[25]

We see the most noticeable improvement in the first excited state angular distributions and those for the two negative-parity states, since in these three cases the most probable and dominant couplings can all be included in the calculations. However, for the two $d_{5/2}$ states we are able to include only a few of several nearly equally important multistep paths, and the improvement over DWBA would not be expected to be dramatic. Since the CCBA calculations do not contain adjustable parameters, we feel that the good fits obtained in both shape and magnitude suggest that CCBA should largely replace DWBA as the primary tool for analysis of experimental data for single nucleon stripping and pickup reactions in this mass region.

An added advantage of CCBA analyses is the light shed on the corevibrational nature of the final nuclear states, through treatment of incident-channel excitations. The nuclear structure information obtained can easily be compared with, or checked for consistency with, nuclear structure calculations available in the literature.

---

*Research supported in part through the U. S. Energy Research and Development Administration.

[1]R. H. Bassel, Phys. Rev. 149, 791 (1966), and references therein.
[2]A. K. Abdallah, T. Udagawa, and T. Tamura, Phys. Rev. C 8, 1855 (1973), and references therein.
[3]W. R. Coker, Phys. Rev. C 9, 784 (1974).
[4]L. Ray and W. R. Coker, Phys. Lett. 56, B318 (1974).
[5]R. Leleux, P. Macq, J. P. Meulders, and C. Pirart, Z. Phys. 271, 139 (1974).
[6]W. R. Coker, T. Udagawa, and G. W. Hoffmann, Phys. Rev. C 10, 1792 (1974).
[7]W. R. Coker, Phys. Rev. C 7, 2426 (1973).
[8]B. Mertins, C. Mayer-Böricke, and H. Kattenborn, Nucl. Phys. A158, 97 (1970).
[9]D. Stupin, R. Ristenen, and P. Schwandt, Nucl. Phys. A173, 286 (1971).
[10]A. Kattenborn, C. Mayer-Böricke, and B. Mertens, Nucl. Phys. A138, 657 (1969).
[11]P. P. Zarubin *et al.*, Izv. Akad. Nauk SSSR Ser. Fiz. 35, 1730 (1971) [Bull. Acad. Sci. USSR Phys. Ser. 35, 1575 (1971)].
[12]M. Berg, A. Hofman, K. Thomas, H. Rebel, and G. W. Schweimer, Phys. Lett. 42B, 211 (1972).
[13]S. A. Fulling and G. R. Satchler, Nucl. Phys. A111, 81 (1968).
[14]W. Fitz, J. Heger, R. Santo, and S. Wenneis, Nucl. Phys. A143, 113 (1970).
[15]F. Kinterberger, G. Mairle, U. Schmidt-Rohr, G. J. Wagner, and P. Tureck, Nucl. Phys. A115, 570 (1968).
[16]G. M. Crawley and G. T. Garvey, Phys. Rev. 160, 981 (1968).
[17]R. Barnard and G. D. Jones, Nucl. Phys. A108, 655 (1968).
[18]G. M. Crawley and G. T. Garvey, Phys. Rev. 167, 1070 (1968).
[19]W. R. Coker, Z. Phys. A273, 251 (1975).
[20]C. M. Perey and F. G. Perey, At. Nucl. Data Tables 13, 293 (1974).
[21]T. Tamura, Oak Ridge National Laboratory Report No. ORNL-4152 (unpublished).
[22]T. Udagawa and T. Tamura (unpublished).
[23]G. Brown, J. G. B. Haigh, and D. L. Watson, Nucl. Phys. A232, 125 (1974).
[24]G. W. Hoffmann, T. Udagawa, W. R. Coker, and J. McIntyre, Phys. Lett. 50B, 249 (1974).
[25]B. H. Wildenthal and J. B. McGrory, Phys. Rev. C 7, 714 (1973).
[26]T. Tamura (unpublished).
[27]E. Rost, Phys. Rev. 154, 994 (1967).
[28]B. Castel, K. W. C. Stewart, and M. Harvey, Can. J. Phys. 48, 1490 (1970).